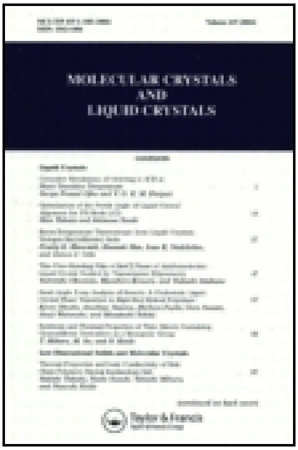

Molecular Crystals and Liquid Crystals Science and Technology. Section A. Molecular Crystals and Liquid Crystals

Publication details, including instructions for authors and subscription information:
http://www.tandfonline.com/loi/gmcl19

An Adaptive Microlens Formed by Homeotropic Aligned Liquid Crystal with Positive Dielectric Anisotropy

Toralf Scharf [a], Joël Fontannaz [a], Manuel Bouvier [a] & Joachim Grupp [b]

[a] Institute of Microtechnology, University of Neuchătel, Rue A.-L. Breguet, 2 2000, Neuchătel, Switzerland

[b] ASULAB S.A. Rue de Sors 3, 2074, Marin-Epagnier, Switzerland

Version of record first published: 04 Oct 2006

Mol. Cryst. Liq. Cryst., 1999, Vol. 331, pp. 235-243
Reprints available directly from the publisher
Photocopying permitted by license only

An Adaptive Microlens Formed by Homeotropic Aligned Liquid Crystal with Positive Dielectric Anisotropy

TORALF SCHARF[a], JOËL FONTANNAZ[a], MANUEL BOUVIER[a] and JOACHIM GRUPP[b]

[a]*Institute of Microtechnology, University of Neuchâtel, Rue A.-L. Breguet 2 2000 Neuchâtel, Switzerland and* [b]*ASULAB S.A. Rue de Sors 3, 2074 Marin-Epagnier, Switzerland*

A novel switchable microlens configuration is proposed and demonstrated. An adaptive microlens system was built with a homeotropic aligned liquid crystal of positive dielectric anisotropy and with a circular electrode structure on one side of a sandwiched liquid crystal cell. The fringing effect at the electrode etches produces spatial distribution of the electric field. Applying a voltage deforms the liquid crystal director field. This produces an axially symmetric profile of the extraordinary refractive index. This director configuration is expected to have lens properties. Under the influence of an electric field, the liquid crystal cell becomes a concave (diverging) lens. The director structure was investigated by polarising microscope. We have simulated the director profile with a finite element method and compared the calculated director profile with the measurements. The properties are discussed from the viewpoint of the director orientation in the spatial non-uniform electric field.

Keywords: liquid crystal; homeotropic alignment; microlens; optical properties; polarisation insensitive

INTRODUCTION.

The use of optical systems where the focal length could be adopted by varying an electric field would help to realise a lot of interesting applications. Liquid crystal lens systems[1,2,3,4,5] offers the potential to do this but the problem of existing LC lenses is their dependence on the direction of polarisation of light. In addition, the anisotropy of liquid crystals in the planar configuration makes obtaining axial symmetric lens systems[10] difficult. As long as these systems are using polarizers, the light intensity is reduced too much by the absorption of the polarizers to use them in daylight applications. In binary systems[6] the problem of the polarisation dependence could be eliminated by an alignment for the liquid crystal which is spatially dependent over the substrate surface, but then a continuous change of the focal length is not possible. The other possibility is the use of homeotropic liquid crystal configurations with a material of negative[11] or positive dielectric anisotropy. We decided on studying the lens properties of the homeotropic configuration with positive dielectric constant material[12]. The stability of this texture under the influence of spatial nonuniform electric fields makes it preferable for us.

EXPERIMENTAL.

The electrode pattern was prepared by a photolithographic method. Holes of different diameters were fabricated in a chromium thin film evaporated on glass substrates. The thickness of the glass was 0.3mm thickness. The other electrode was a ITO (indium tin oxide) coated glass plate of 0.55mm thickness with a SiO_2 protection layer from BALZERS. Fig. 1 shows the electrode configuration with the hole in the top electrode. The homeotropic alignment was made by using the polymer RN 722 from NISSAN on both substrate surfaces. This assures strong homeotropic anchoring conditions. The cell thickness d was controlled with glass rod spacers. The resultant thickness was d= 22μm. We used the nematic liquid crystal E7 from MERCK, which has a positive dielectric anisotropy of $\Delta\varepsilon=8$ ($\varepsilon_{\perp}=7$) and a birefringence of $\Delta n=0.199$ ($n_o=1.51$). After sealing and vacuum filling at room temperature, the cell showed homeotropic alignment.

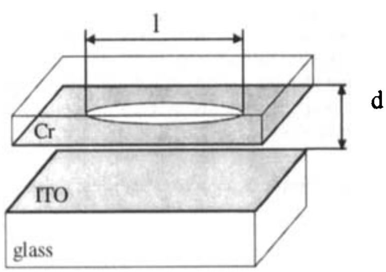

Fig. 1 The electrode structure of the system under investigation. The cover glass has a thickness of 0.3mm with a structured chromium electrode and a hole diameter l between 50 and 120μm.. The bottom glass substrate with unstructured ITO electrode has a thickness of 0.55mm. The thickness of the liquid crystal layer was d=22μm.

Director distribution and imaging properties.

We have investigated the director distribution under crossed polarizers and circular polarised light with a polarising microscope and an interference filter for green light (λ=550nm). When a voltage is applied between the electrodes, various fringes appear. Between crossed polarizers, full extinction is observed along the direction of the polarizers orientation. If the sample is rotated, no change is visible. This indicates an axial symmetry of the director distribution. Therefor the analysis of the intensity distribution becomes straightforward.

In circular polarised light, the intensity is independent of the position of the optical axis[9]. The fringes give directly the distribution of the effective birefringence Δn_{eff}. The effective birefringence depends only on the tilt angle Θ of the director. When the voltage is varied, the fringes change in diameter and appearance. This is due to the change of the director structure by the fringing fields at the edges of the electrodes. Fig. 2 shows photographs of the fringes for an applied AC voltage at a frequency of 20 Hz for a lens diameter of 120µm in circular polarised light. The fringing fields start at the edges for low voltages and influence the centre only at very high voltage levels. The circular symmetry does not change. In general, only 3 or 4 fringes are visible at once, therefor the phase shift is small compared to conventional lens systems. No defects appear during the change of the voltage. The radial symmetry of the director distribution makes the lens invariant to the direction of

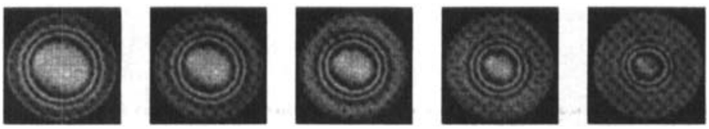

10V 15V 20V 30V 50V

Fig. 2 Photograph of the fringes appeared under the polarising microscope in circular polarised green light (λ=550 nm). The diameter of the structure is 120µm and cell thickness 22µm.

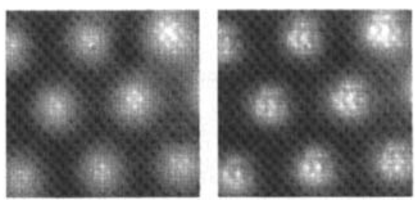

Fig. 3 Imaging with homeotropic microlenses of 90µm diameter and 22µm thickness. The left picture is without applied voltage and the right with 50V (20Hz rms) applied at the electrode. The picture was taken without polarizers under the microscope (magnification 20x).

the polarisation. The distribution of the extraordinary refractive index is responsible for the focusing effect. The ordinary refractive index does not influence the optical properties, therefor the maximum intensity of the lens function is only 50% of the full intensity.

The imaging properties of an array of a microlenses in white light are shown in Fig. 3. The distortion of the director field due to the spatial nonuniform electrical field gives a divergent lens. The imaging quality of the system is worse compared to conventional microlenses.

THEORETICAL BACKGROUND.

Simulation of the director field.

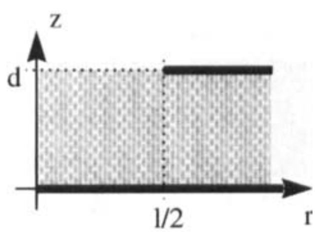

Fig. 4 NLC cell geometry of the simulation with circular symmetry (cylindrical coordinate system). The whole diameter is l/2 and the thickness of the cell d.

The nematic liquid crystal cell geometry for simulation is shown in Fig. 4. The cell includes the electrodes with the hole on top and another electrode of infinite size on bottom. The radius of the hole is l and the cell thickness d. The director profile of the nematic liquid crystal was simulated in two steps. At first the electric potential was calculated by solving the LAPLACE equation. Then, the equation for the director profile was solved by taking the spatial nonuniform electrical field into account. The calculations were made with a finite element method using MATLAB.

The equation for the electric potential u(r,z) in cylindrical coordinates for axial symmetry is

$$\varepsilon_{\perp}\frac{\partial}{\partial r}r\frac{\partial u}{\partial r}+(\Delta\varepsilon+\varepsilon_{\perp})r\frac{\partial^2 u}{\partial z^2}=0 \qquad \text{Eq. 1.}$$

where $\varepsilon_{\perp}$ and $\Delta\varepsilon$ are the dielectric constants perpendicular to the director and the dielectric anisotropy respectively. In the electrode area, in Fig. 4 z=d and r>l/2, the electrical potential fulfils the boundary condition $u|_{|r|>l/2}=u_0$, where u_0 is the applied potential at the electrode. For the electrode free area (r<l/2 and z=d) one has $\frac{\partial u}{\partial z}=0$. For the bottom electrode the potential is zero, hence

$u|_{z=0} = 0$. For the simulation parameters u_0=2, d=20μm, l=70μm, ε_0=8.85 10^{-12}As/Vm and Δε=8 are chosen, the resulting electrical field distribution is shown in Fig. 5. Due to the structure of the Eq.1 one always gets a similar shape of the electrical field and only the absolute values of u change.

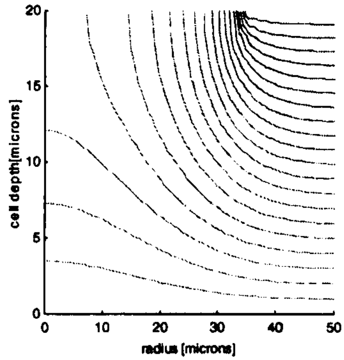

Fig. 5 Electrical field distribution as isopotential lines in the NLC. l=70μm, d=20μm, u=2 d=20μm, E7. The lines are specifying the potential form 0 to 2 with 20 levels starting at cell depth 0.

The calculation of the director distribution is made for small angle deviations from the initial director orientation. With the coordinate system specified in Fig. 6, the director **n** is defined as $n = \lfloor \sin\Theta \quad 0 \quad \cos\Theta \rfloor$ in cylindrical coordinates. With the assumption of small tilt angles Θ, one gets $n = \lfloor \Theta \quad 0 \quad 1 \rfloor$. This is valid for tilt angles Θ smaller than one half. If the tilt angle Θ is larger, the electric field distribution cannot assumed to be fixed by the director reorientation and the approximation reaches the limit of validity. The director field is determined by the minimum of the nematic liquid crystal free energy. Therefor, the deviation angle Θ(r,z) of the director from the initial homeotropic orientation is defined by the EULER LAGRANGE equation. One finds in our special case[7,8] by neglecting flexoelectric contributions:

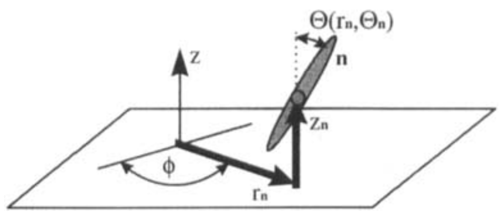

Fig. 6 Definition of the three dimensional director description in cylindrical coordinates. The system is independent of the azimuthal angle φ.

$$k_{11}\frac{1}{r}\frac{\partial}{\partial r}r\frac{\partial\Theta}{\partial r} + k_{33}\frac{\partial^2\Theta}{\partial z^2} + \Delta\varepsilon\varepsilon_0 E_r E_z = 0 \qquad \text{Eq. 2}$$

where k_{11} and k_{33} are the splay and bend elastic constants, respectively. Due to the axial symmetry of the problem no twist deformation occurs. E_z and E_r are

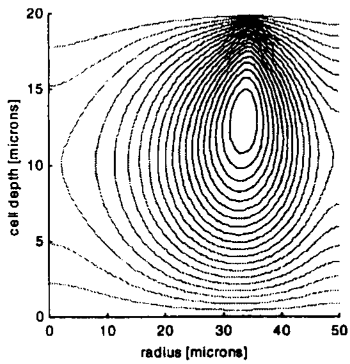

Fig. 7 Isolines of the director profile. The dimensions are d=20mm, l=70mm. The potential is u=2. The lines are indicating the values from 0 to 0.7 with 20 levels starting at the boundary.

the electric field components $E_z = -\frac{\partial u}{\partial z}$ and $E_r = -\frac{\partial u}{\partial r}$. The dielectric coupling is described by the dielectric anisotropy $\Delta\varepsilon$. At the substrate surfaces, strong anchoring is assumed, i.e. at z=0 and z=d the tilt angle Θ has to be zero: $\Theta|_{z=0} = 0$, $\Theta|_{z=d} = 0$. For the other two borders, boundary conditions were used with a vanishing derivation normal to the surface. The flexoelectric effect was neglected in the calculations because of the use of high voltages[7]. With d=20μm, l=70μm, $\Delta\varepsilon/\varepsilon_{||}$=0.5 and the one constant approximation $k_{11}=k_{33}$=15pN the director field distributions are calculated as shown in Fig. 7. The potential is u=2. The maximum value of the electric potential is limited by the condition of the value of Θ. For values larger than u=2 one gets tilt angles Θ which do not fulfil the condition of the small Θ approach. This is one disadvantage of the approach, because the potential u=2 is relatively low. But the parameter dependence for discussing the influence of the dielectric constant and the elastic constant does not change.

The most important quantity for characterising LC lens properties is the value of the birefringence. The spatial distribution of the local birefringence is calculated by using the tilt angle Θ and the formula of the effective refractive index[8]

$$n_{eff}(r,z) = \frac{n_o n_e}{\sqrt{n_e^2 \cos^2\Theta(r,z) + n_o^2 \sin^2\Theta(r,z)}} \qquad \text{Eq. 3.}$$

The effective birefringence is given by the integration over the cell thickness :

$$\Delta n_{eff}(r) = \frac{1}{d}\int_0^d n_{eff}(r,z)\,dz - n_o \qquad \text{Eq. 4.}$$

The absolute relative phase shift between the extraordinary and the ordinary beam for a birefringent plate is then $\Delta n_{eff}\, d/\lambda$. Since the optical path during observation is much larger than the cell thickness, the optical properties of the lens are described by the phase shift.

DISCUSSION.

The change of the phase shift for different potentials indicates the mechanism how the fringing electrical field performs the lens properties. In the centre of the lens system, for small r, one always has a small dependence of the phase shift on the radius. The phase shift is increasing with increasing radius, which gives divergent lens properties. Close to the edges of the patterned electrode (radius=35μm in Fig. 8), the derivation of the phase-shift-radius curve changes sign. Therefor, a convex like lens property appears in the area outside the hole. According to Eq 2. the influence of the electric field on the deformation of the director field is controlled by the square of the electrical field and the value of the parameter $\varepsilon_0 \Delta\varepsilon / k_{11}$. The electric field distribution itself is also determined by the dielectric anisotropy $\Delta\varepsilon$. For a given electrical field, it is evident that the director deformation is stronger for a smaller elastic constant k_{11} and a higher dielectric anisotropy $\Delta\varepsilon$. Due to the structure of Eq 1., one always gets a similar shape of the electrical field and only the absolute value of the potential changes. Since Eq 1. and Eq 2. have the same structure, there is the same behaviour for both concerning the shape of the field distributions. Therefor the director field has also a similar shape for different values of the electric potential, although the absolute values of the tilt angles are different. If the shape of the director distribution remains similar for different potentials, the distributions of the birefringence are self similar to each other, although the effective birefringence vary in magnitude and provides different focal lengths. As the lens errors are determined by the

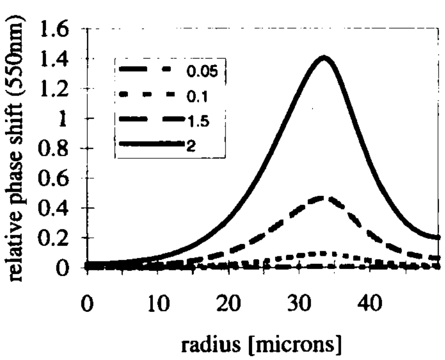

Fig. 8 The simulated relative phase shift for different potential u. n_e=1.7 ,n_o=1.5, d=20μm and l=70μm, E7.

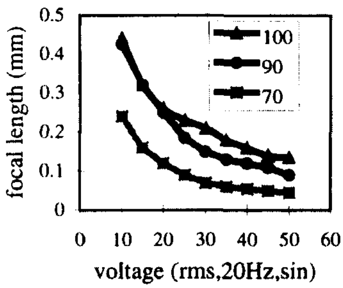

Fig. 9 Voltage dependence of the focal length of homeotropic liquid crystal microlenses with different hole diameters. 70μm,90μm and 100μm in chromium.

spatial distribution of the birefringence, they cannot be eliminated. The ideal shape of the birefringence distribution would be a quadratic dependence of the phase shift on the radius. For the potentials simulated in Fig. 8 this is not well fulfilled. This modelisation gives indeed a simplified picture of the situation but means on the other hand, that the improvement of the calculation needs a model for large tilt angles and the knowledge of the flexoelectric contributions.

The experimental results are visible in Fig. 3, where the bad quality of the imaging is documented. The optical quality of the lens systems was also tested by using a MACH-ZEHNDER interferometer. The phase profile of an incident plane wave was evaluated. The quality standards of micro-optical elements will not be reached with such a system. The wavefront modulation showed a lot of aberrations, because the phase deviation is high compared with an ideal lens.

The measurements of the focal length are given in Fig. 9. For the diameters of 70μm, 90μm and 100μm the focal length was measured with a microscope[14]. The values of the focal length for the lens systems with smaller diameters were smaller at the same voltage. With increasing voltage the focal length always decreases. This is due to the larger phase shift introduced by a stronger deformation of the director field as indicated in Fig. 8. The measured focal length changes from infinity at zero voltage to 0.2mm for the 70μm diameter lens and to 0.3mm for the 90μm diameters at $50V_{rms(20Hz)}$.

CONCLUSION.

A LC microlens with a homeotropic liquid crystal configuration and positive dielectric anisotropy was built. The system has variable focal length and is invariant to the rotation of the polarisation direction. No disinclination lines were observed. It was found that the imaging properties are relatively bad compared to conventional lenses. The spatial distribution of the phase shift was simulated for small deviations from the homeotropic configuration and could explain the optical properties for low voltages. An improved model for simulating the director distribution has to take into account large tilt angles and the flexoelectric effect.

Acknowledgements.

We thank Reinhard Völkel for the investigations at the MACH-ZEHNDER interferometer and for useful discussions.
Our work was supported by the Swiss Priority Program Optique II.

References

[1] S. SATO: Liquid-Crystal Lens- Cell with Variable Focal Length. Jpn.J.Appl.Phys. 18 (1979) pp. 1679–1684.

[2] T. NOSE, S. MASUDA AND S. SATO: Optical Properties of a Liquid Crystal Microlens with a Symmetric Electrode Structure. Jpn. J. Appl. Phys. 30(1991)pp.L2110-L2112.

[3] M.FERSTL, A.FRISCH: Switchable Fresnel zone lenses for optical interconnections. SPIE Vol. 2881 (1996) pp.141–147.

[4] H. MOLSEN, J. ESCHLER AND D.A. MLYNSKI: Fast Adaptive Lens based on Deformed Helical Ferroelectric Liquid Crystal. Freiburger Arbeitstagung Flüssigkristalle 1995, pp. 215–216.

[5.] L.G. COMMANDER, S.E. DAY AND D.R. SELVIAH: Electrode design for tunable microlenses, EOS Topical Meeting 1997, Abstract M.1.7, pp.48–53.

[6] J.S. PATEL AND K. RASTANI: Electrically controlled polarization independent liquid-crystal Fresnel lens arrays. Optics Letters 16 (1991) pp.532–534.

[7] L.M. BLINOV, V.C. CHIGRINOV: Electrooptic Effects in Liquid Crystal Materials. Springer, Berlin New York 1996. pp. 284–291.

[8] G.E. NEVSKAYA, V.V. KORNILOV, O.V. MAKAROVA, V.G. CHIGRINOV: Investigation of NLC deformations in a nonuniform electric field. SPIE Vol. 2731 1996 pp.28–34

[9] S. HUARD: Polarisation de la lumière. Masson Paris 1994.

[10] S. MASUDA, M. HONMA, T. NOSE AND S. SATO: Influence of Elastic Constants on the Optical Properties of Liquid Crystal Microlenses. Jpn. J. Appl. Phys. 36(1997) pp.2765–2770.

[11] A. GWOZDAREV, G.E. NEWSKAJA: Homeotropical-aligned liquid crystal microlens properties. SPIE Vol.2731 pp.214–219.

[12] J.H. KULICK, J.M. JAREM, R.G. LINDQUIST, S.T. KOWEL, M.W. FRIENDS AND T.M. LESLIE: Electrostatic and diffraction analysis of a liquid-crystal device utilizing fringing fields: application to three-dimensional displays. Applied Optics 34(1995) pp.1901–1922.

[13] R. VÖLKEL: unpublished results.

[14] G. SCHRÖDER: Technische Optik. Vogel Würzburg 1990.